Investigation into starting speed of stone in slurry shield circulation system

Chengyuan Wu

Kangqiao Campus of Hangzhou No.14 Middle School, Hangzhou,China

2148812945@qq.com

Abstract. Slurry circulating system is the core system for transporting excavated stone from the excavation interface, and the flow characteristics of stone in circulating pipeline is the key to determine whether stone can be transported smoothly. Based on Computational Fluid Dynamics-Discrete Element Method (CFD-DEM) coupling method, the movement model of stone in horizontal straight pipe of circulation system is established, and the influence of stone shape coefficient and equal volume particle size on stone starting speed is studied. The simulation results indicate that under the condition of equal volume particle size of stone is same, starting speed of stone with different shapes is ellipsoid > flat > nearly spherical; When the equal volume particle size of stone is 38.5, 42.5, 53.3, 56.2 and 58 mm, the starting speed of stone is 0.48, 1.06, 1.26, 2.36 and 4.7 m/ s respectively, which increases exponentially with the increase of equal volume particle size. The conclusions can be helpful for setting the working parameters of circulation system.

Keywords: Slurry shield circulation system; starting speed; CFD-DEM method; Non-Newtonian fluid.

1. Introduction

1.1 Background

With the continuous growths of the number of urban underground space and cross-river-sea tunnel projects in my country, the mud-water shield construction technology has been more and more widely used [1-2]. The slurry shield circulation system working diagram is shown in Fig. 1. The circulation system, as the core system of slurry shield to transport the stone, is prone to a series of problems such as rock accumulation, blockage of the quarry box and insufficient energy supply of the slurry pump during the excavation of the rock formation. The critical state in which the particles change from static to moving is called particle starting. Studying the starting characteristics of stones in pipe is beneficial to reduce the energy waste of circulation system and reduce the occurrence of massive accumulation of stones.

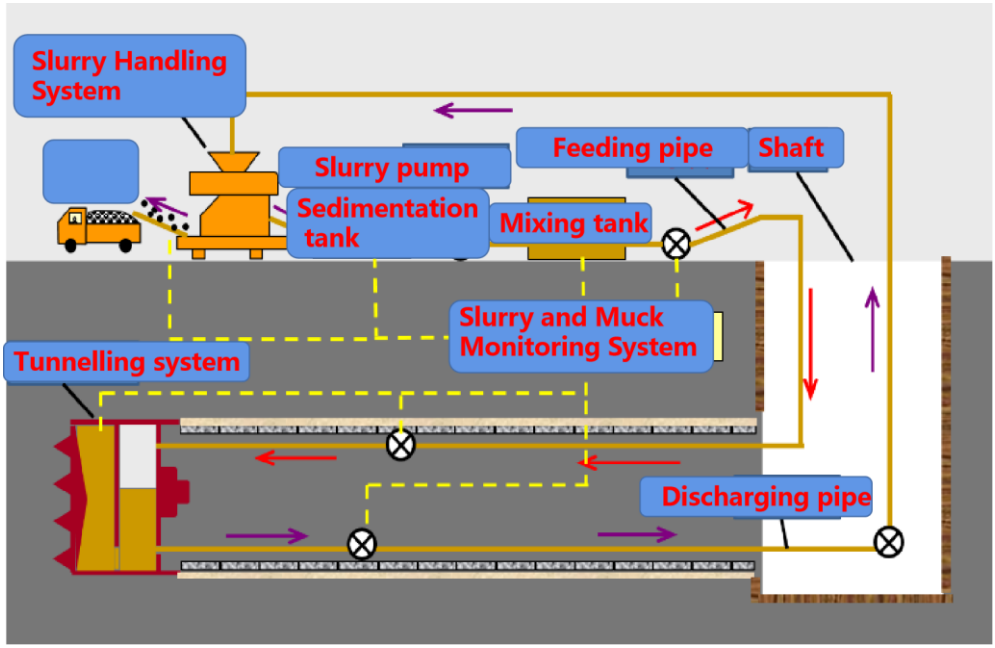


Figure 1: Slurry shield circulation system working diagram.

1.2 Literature review

At present, many scholars have carried out a series of related researches on the transport characteristics of particles in the pipeline. Yang et al. [3] took the Lanzhou subway river-crossing tunnel project as the research background, and used the numerical simulation means to establish a slurry-stones flow model of debris flow, considering the rheological characteristics of the slurry, and studied the multi-phase flow theory. Corresponding simulation models for experimental verification were established via utilizing CFD and DEM software, and the effects of entrance mud flow rate, ballast volume fraction and pipeline inclined angles on pipeline pressure drop and carrying ability were studied. Tan [4] and Zhang et al. [5] employed the DEM to forecast the motion trajectories and particle-particle interactions of discrete particles, used the Navier-Stokes solver to evaluate the movement of the uninterrupted liquid phase, and used pressure gradient model to compute the solid-liquid interplay force. Wu et al. [6] established an indoor pipeline circulation transportation system, and studied the transportation characteristics and pressure loss of CGFB mud, and discovered that solids content in CGFB mud and the mixing proportion of other components have marked influences on pressure losses of pipeline transportation. Arolla and Desjardins [7] proposed a method for predicting the physical properties of turbulent fluid-solid two-phase slurry flow in pipelines using Eulerian-Lagrangian simulations, which can accurately mean the velocity and mean flowwise pressure gradient. Kaushal et al. [8] used the mixed two-phase flow and Eulerian two-phase flow models in Fluent respectively to calculate and analyze the pressure loss in pipeline transportation of slurries with different concentrations. The results show that the mixed two-phase model cannot accurately predict the pipeline pressure loss, and the error varies with the slurry. The increase in concentration increases rapidly, and the Eulerian model is very accurate for the prediction of mud pressure loss at all concentrations. Akhshik et al. [9] investigated the impact of particle shape on drilling carry idiocratic via CFD-DEM coupling means. Wang et al. [10] used two-way coupling of FEM-DEM to check the characteristics of anomalistic ballast flow in mud circulation system in the process of tunneling. The ballast size of 17~32 mm under various mud velocities and ballast particle volume concentrations was studied to determine the impact law of mud velocities, retention quality percent and ballast distribution. The results show that increasing mud velocities and ballast volume density will increase quality flow rate. The increase of mud velocities and ballast volume density will both reduce the retention quality percent in the mud discharge pipe, while increasing the ballast size will have the contrary effectiveness.

1.3 Section overview

Most of the particle sizes studied by the above scholars are less than 20 mm, and the spherical particle model is also used in the simulation, and there are many studies on the pressure loss and pressure gradient of pipeline transportation. At present, there are no research results on the conveyance of large anomalistic stone in the circulation pipeline. In this paper, aiming at the large-diameter (maximum axis distance: 30-90 mm) irregular stone ballast in the circulation system, taking the horizontal straight pipe at the entrance of the slurry pipe as the research object, the CFD software combined with the DEM is used to study the stone slag. The influence of stone shape factor and equal volume particle size on the starting speed of ballast.

2. Theoretical basis

The implementation of FUENT-EDEM coupling calculation is based on CFD-DEM coupling method, and its calculation process is as follows: point-to-point coupling of boundary grid points of flow field grid in FLUENT and boundary grid points in EDEM, in one time step, the fluid flow field parameters are calculated in FLUENT based on CFD method, and the flow field parameters are converted into drag force information of discrete particles in EDEM by coupling function. Based on DEM method, the force and motion of discrete particles are solved, and the solved particle velocity and position parameters are converted into momentum information of FLUENT flow field by

coupling function, and the next step iterative calculation of flow field is carried out, and the calculation procedure is depicted in Fig. 2. The FLUENT-EDEM coupling calculation not only possess the powerful CFD simulation function of FLUENT software, but also includes the accurate simulation ability of EDEM software for discrete particles, and has good adaptability and accuracy for the simulation calculation that needs to consider the particle shape, self-rotation and collision among particles. According to the requirements of simulation calculation in this chapter, the FLUENT-EDEM coupling calculation method is selected for simulation.

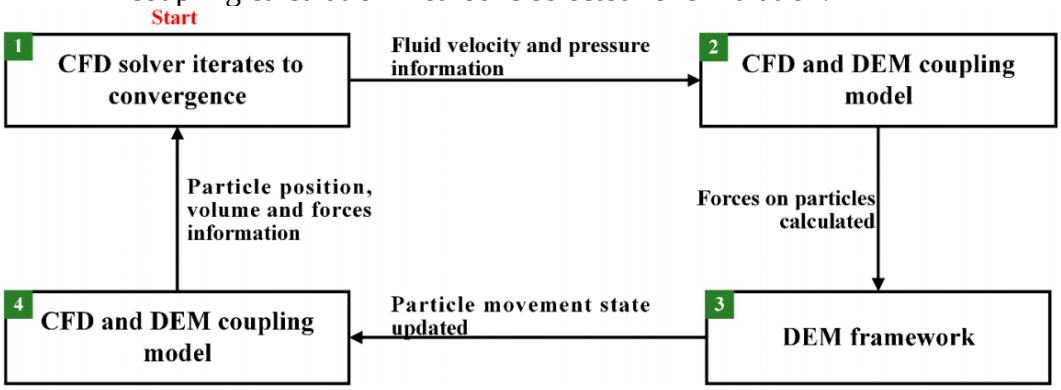


Figure 2: FLUENT-EDEM coupling calculation process. Picture from [10].

2.1 CFD model

The procedure of liquid flow and heat transfer adheres to the law of conservation of quality, momentum and power, and their theoretical models are continuity equation, Navier-Stokes equation and energy conservation equation, as below:

$$\frac{\partial \alpha\rho}{\partial t}+\nabla\cdot(\alpha\rho\mathbf{U})=0 \tag{1}$$

$$\begin{aligned}&\frac{\partial}{\partial t}(\alpha\rho\mathbf{U})+\nabla\cdot(\alpha\rho\mathbf{U}\mathbf{U})\\&=-\nabla p+\nabla\cdot\alpha\tau+\alpha\rho\boldsymbol{g}+\boldsymbol{F}_p\end{aligned} \tag{2}$$

$$\begin{aligned}&\frac{\partial}{\partial t}(\alpha\rho T)+\nabla\cdot(\alpha\rho\mathbf{U}T)\\&=\nabla\cdot\left(\frac{k_T}{c_P}\nabla T\right)+s_T\end{aligned} \tag{3}$$

where α, ρ, U and p are volumetric fraction, density, velocity vector and pressure component of fluid, τ is gummy stress tensor; g is local acceleration of gravity, taking 9.81 m/s2, and Fp is force inflicted by all rock slag on the fluid, T is temperature, kT, cP is heat transmission coefficient and the liquid specific heat capacity, sT is gummy consumption phase.

The slurry used in shield tunnel is a mixture of water, Na-bentonite and slurry making agent. The mixed slurry is effective in increasing the adsorption among particles, thus increasing the slurry shear viscosities, reducing the volume of slurry penetrating into the strata, and making an important contribution to maintaining the excavation face consistency. Taking mud from the construction site as the sample, rheological curves of Na-bentonite mud are given via utilizing the coaxial cylindrical measuring device CCT-40 and the blade measuring device VT-40-20. Herschel-Bulkley rheological model is used to fit the two groups of test data well, not Bingham model, especially in the lower shear rate ranges. This phenomenon is mainly due to the shear dilution characteristics of mud as solid-liquid two-phase fluid. Herschel-Bulkley model is often used to describe fresh concrete, slurry, suspension

containing particles and other materials because of its wide applicability. The correlation between shear stress and strain rate could be expressed as follows:

$$\tau = \tau_0 + k\dot{\gamma}^n \qquad (|\tau| > \tau_0) \tag{4}$$

$$\dot{\gamma} = 0 \qquad (|\tau| \le \tau_0) \tag{5}$$

where is τ0 yield stress, k is viscosity coefficient, and n is power law index. When n=1, Herschel-Bulkley model is Bingham model. The Herschel-Bulkley plastic viscosity coefficient, yield stress and power-law exponent of the bentonite mud samples are 0.766 Pa·sn, 4.338 Pa and 0.601, respectively. The H-B rheology of the bentonite slurry can be directly entered into the CFD software. Due to large pipe sizes and high flow rates of mud and slag in the pipe, the Reynolds number Re is more than 2300, so mud flow in the discharge pipe is standard turbulence. In this simulation, the widely used k - Epsilon double equation turbulence model for calculation. The equations are as follows:

$$\begin{cases} \dfrac{\partial(\rho\kappa)}{\partial t} + \dfrac{\partial(\rho\kappa u_i)}{\partial x_i} = \dfrac{\partial}{\partial x_j}\left[(\mu + \dfrac{\mu_t}{\sigma_\kappa})\dfrac{\partial\kappa}{\partial x_j}\right] + G_\kappa - \rho\varepsilon \\ \dfrac{\partial(\rho\varepsilon)}{\partial t} + \dfrac{\partial(\rho\kappa u_i)}{\partial x_i} = \dfrac{\partial}{\partial x_j}\left[(\mu + \dfrac{\mu_t}{\sigma_\varepsilon})\dfrac{\partial\varepsilon}{\partial x_j}\right] + \dfrac{C_{1\varepsilon}\varepsilon}{\kappa}G_\kappa - C_{2\varepsilon}\rho\dfrac{\varepsilon^2}{\kappa} \\ \mu_t = \rho C_u \dfrac{\kappa^2}{\varepsilon} \end{cases} \tag{6}$$

where the κ is turbulence energy, ε is turbulence dissipation rate, μ_t is turbulence viscosity.

2.2 DEM model

In the process of pipeline conveying, the stone is affected by other stones, mud and tube wall, which could be indicated via Newton's second law of movement, via DEM initially presented by Cundall and Strack [12], as below:

$$m_i \frac{d\boldsymbol{U}_{p,i}}{dt} = m_i\boldsymbol{g} + \sum_{j=1}^{n}(\boldsymbol{F}_{c,ij} + \boldsymbol{F}_{d,ij}) + (\boldsymbol{F}_{c,iw} + \boldsymbol{F}_{d,iw}) + \boldsymbol{F}_{f,i} \tag{7}$$

$$\boldsymbol{I}_i \frac{d\omega_i}{dt} = \sum_{j=1}^{n}\boldsymbol{T}_{ij} + \boldsymbol{T}_{iw} \tag{8}$$

where m_i, $Up_{,i}$, I_i, ω_i are the quality velocity, inertial movement and rotational speed of particle i; $F_{c,ij}$, $F_{d,ij}$ and T_{ij} are the interparticle contact forces, adhesive frictional forces and Moments; $F_{c,iw}$, $F_{d,iw}$, and T_{iw} are the contact forces, adhesive frictional forces and torque between particle i and the tube wall. $F_{f,i}$ is force inflicted by the liquid phase on particle i.

Due to the large difference in the geometry of the rock slag in mud discharge pipe of mud-water shield, the irregular rock slag with a particle size larger than 20 mm discharged from the slurry discharge pipe is now screened and sampled according to the order of magnitude. In order to determine more accurately The starting speed of the stone, using a white light object 3D scanner to scan the geometric model of the special-shaped stone, the special-shaped stone model is described in Fig. 3. It can be obtained from the Fig. 3 that the shape of the stone has three shapes: flat, ellipsoid and nearly spherical, and the size of stone is also different. For the convenience of discussion, the shape and size of the stone is characterized by the shape coefficient and equal volume particle size of the stone, as shown in formula (9) and (10):

$$S_f = \frac{c}{\sqrt{ab}} \tag{9}$$

$$D_V = (6V_S / \pi)^{1/3} \tag{10}$$

where S_f is the shape coefficient of stones, a, b, and c are the lengths of the three axes of the stone, a is the longest axis distance, and c is the shortest axis distance. When S_f is less than 0.4, the stone is flattened; when S_f is between 0.4 and 0.8, the stone is ellipsoidal; when S_f is greater than 0.8, the stone is subspherical. D_V is the equal volume particle size of stones, V_S is true volume of stones.

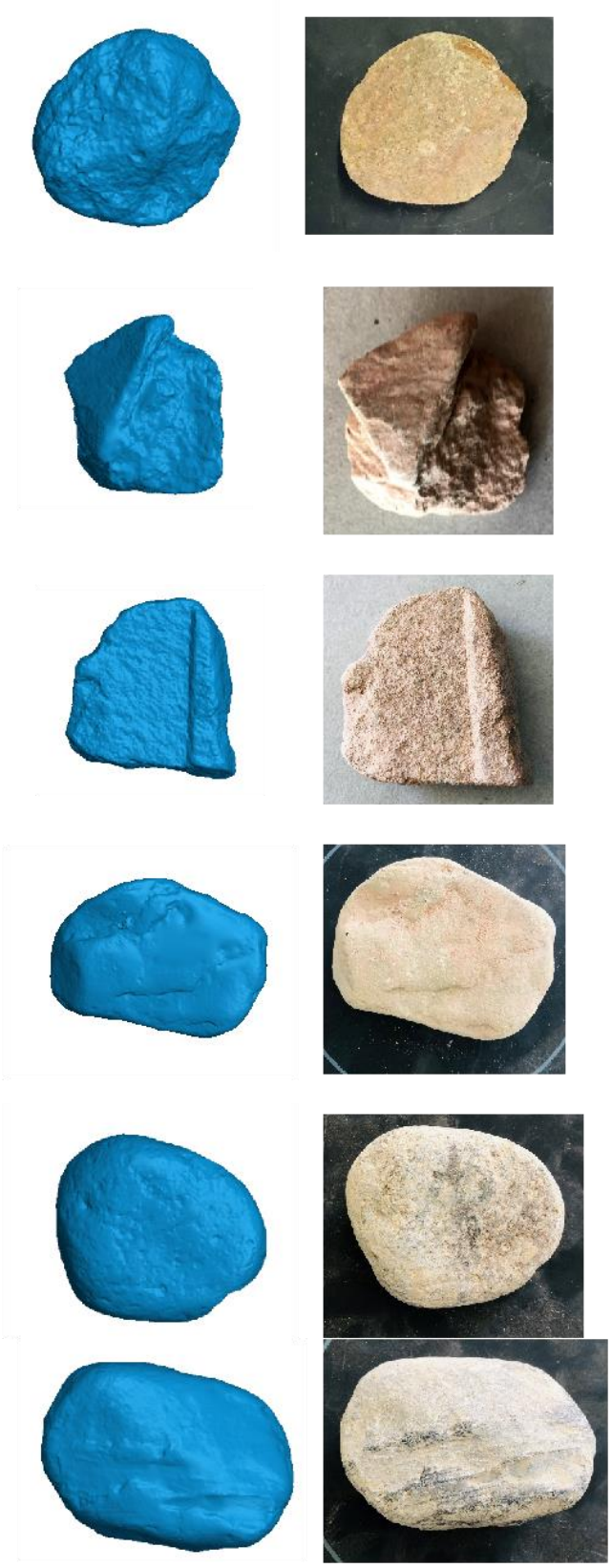


Figure 3. Numerical geometric modeling of irregular stones obtained via the 3D scanning.

2.3 Interactions between stone particle and fluid

The interactions between the slag and the fluid is mainly composed of buoyancy F_B, drag force F_D and pressure gradient F_P. The calculation formulas for above forces are as follows:

$$\boldsymbol{F}_b = -\frac{\rho_f}{\rho_p}\boldsymbol{g} \tag{10}$$

$$\boldsymbol{F}_d = \frac{18\mu}{\rho_p d_V^2}\frac{C_D Re_p}{24}(\boldsymbol{U}_f - \boldsymbol{U}_p) \tag{11}$$

$$\boldsymbol{F}_p = -\frac{1}{\rho_p}\nabla p_f \tag{12}$$

where ρ_P is the stone density, d_V is the diameter of the equivalent volume spheres, μ is liquid viscosity, C_D is resistance coefficient, and *Rep* is stone Reynolds number.

2.4 Setting of geometric model and boundary conditions

The horizontal pipeline is 5 m long and 300 mm in diameter. The geometric model is shown in Figure 4. To study the starting speed of stone, that is, the speed at the moment when stone changes from static state to moving state, stone is placed in the pipeline with a density of 2700 kg /m^3 and a slurry density of 1200 kg /m^3, and the uniformly accelerated slurry inlet velocity is set. Its UDF is v_m = 2t m/s. It can be concluded that the starting time t_s of stone under different parameter changes (corresponding to the inflection point on the speed curve), and the starting speed v_i of ballast is equal to $2t_s$ m/s. The boundary conditions are velocity inlet condition, total pressure outlet boundary condition and wall non-slip condition. And the Phase Coupled SIMPLE algorithm is used to address the coupled equations of velocity and pressure.

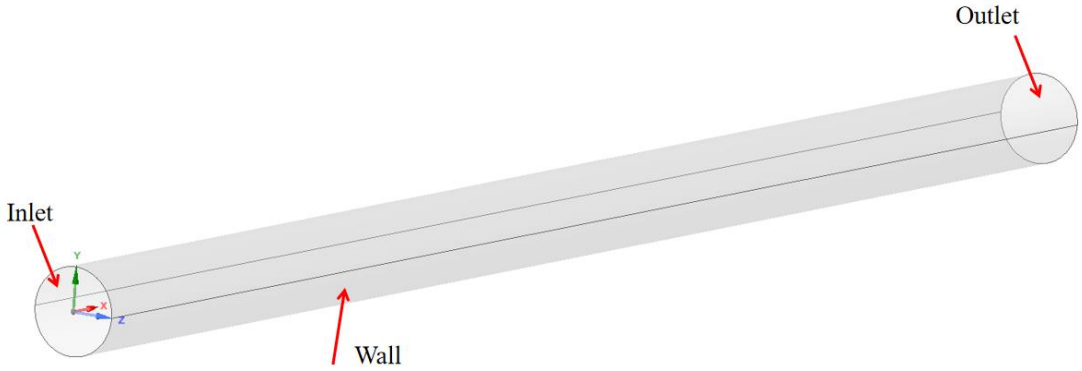


Figure 4. Geometrical model.

3. Numerical results and discussion

3.1 Influence of shape coefficient on starting speed of stone

To investigate the affect of shape coefficient on starting speed of stone particles, a single ballast with equal volume particle diameter D_V = 38.5 mm was placed at the bottom of the pipeline at a certain distance from the inlet surface. The starting speed of ballast with different shape coefficients is illustrated in Fig. 5. Fig. 5 illustrates that when the shape coefficient S_f of stone is 0.2 ~ 0.37 and 0.8 ~ 0.94, the starting speed of ballast decreases with increasing shape coefficient, the maximum starting speed of ballast is 0.589 m/s and 0.2 m/s respectively. When the shape coefficient S_f = 0.55, compared with the shape coefficient S_f = 0.37, the starting speed of the stone jumps, reaching 1.4 m/s, with an increase of 204%. The angular velocity of ellipsoidal ballast (S_f = 0.72) is described in Fig. 6. It can be obtained from Fig. 7 that the angular velocities of stone in X and Y directions is large, and the angular velocity in X direction is obviously larger than that in Y direction. The maximum angular velocity in X direction is 0.75 rad/s, while that in Y direction is only 0.11 rad/s, and that in Z direction is almost zero. The angular velocity in X and Y directions vibrates up and down at 0 o'clock,

and the amplitude of vibration gradually decreases with the increase of time, and finally tends to 0. This time is 0.69 s, which is the starting time of stone. It can be concluded that before 0.69 s, the ellipsoidal ballast rotates around the X and Y directions, and the movement around the X direction is more intense, and it starts after 0. 69 s.

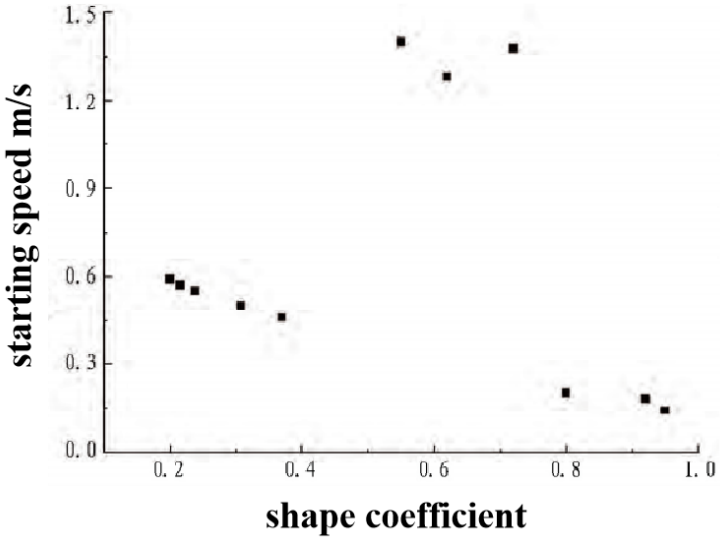


Figure 5. Starting speed of stone under different shape coefficients.

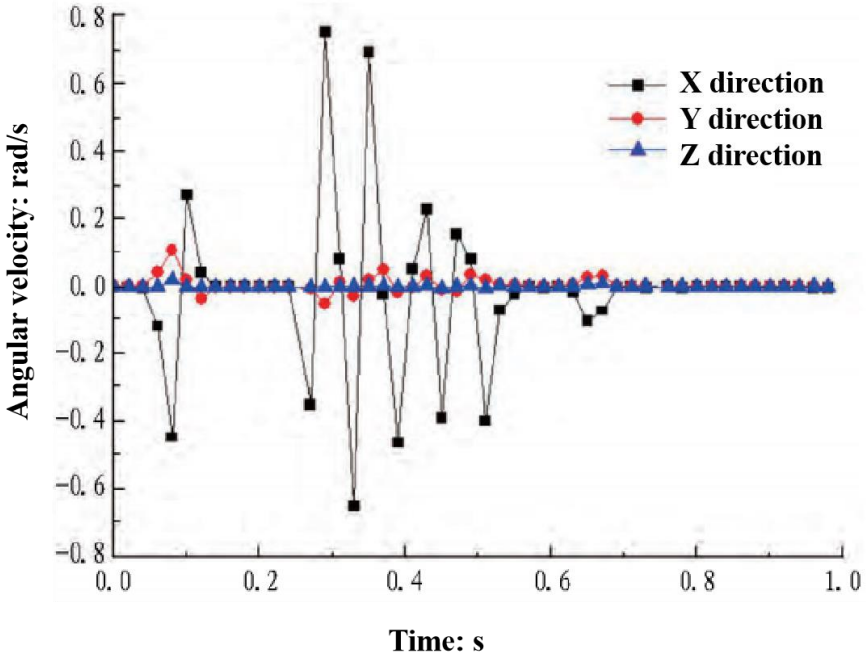


Figure 6. Angular velocities of a stone with axiolitic shape (Sf =0.72).

The angular velocity of the flat stone (S_f = 0.37) is depicted in Fig. 7. It can be depicted from Fig. 7 that the angular velocity of the stone in the X, Y and Z directions is not large, the angular velocity in the X and Z directions is almost zero, and the angular velocities in the Y direction is 0 ~ 0.01 rad/s. Thus, the flat stone hardly moves in rotation, but only moves along the pipeline axis with the increase of drag force.

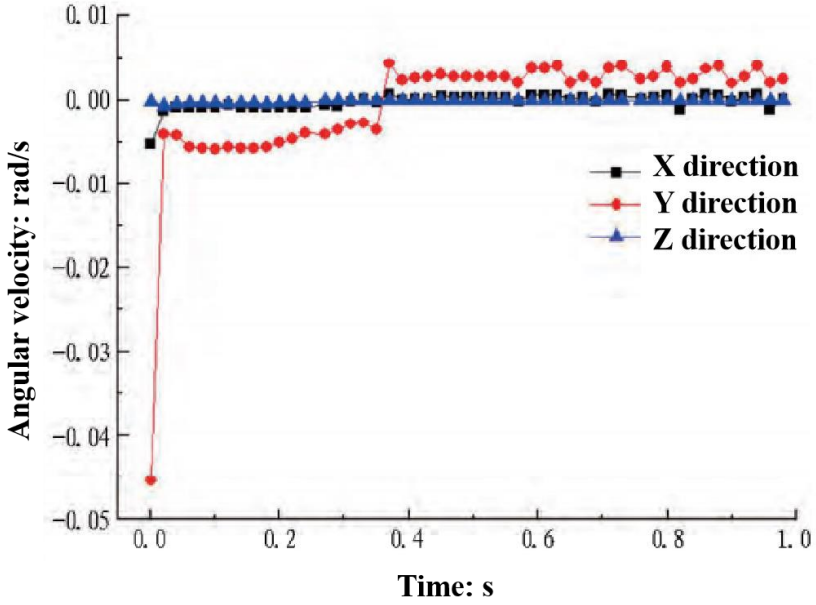


Figure 7. Angular velocities of a pebble with flat shape(Sf = 0.37).

The angular velocity and movement speed of two kinds of stone are depicted in Fig. 8 and Fig. 9. It can be depicted from the figure that the motion state of the two kinds of stone before starting is different. The ellipsoidal stone rotates to a certain extent, while the flat stone is almost at rest.

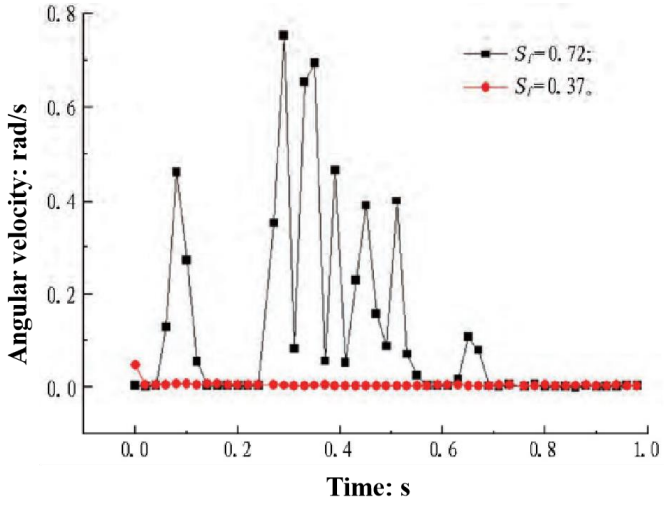


Figure 8. Angular velocities of two kinds of shape stones.

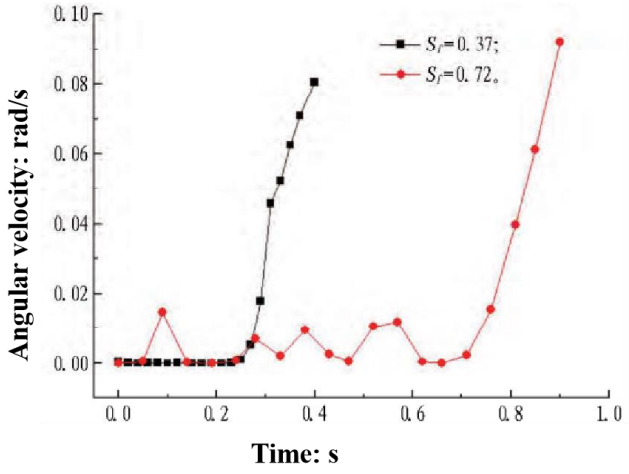


Figure 9. Velocities of two kinds of stones.

Stone can be divided into three different starting conditions. When the shape of the stone is flat, the movement form of the stone is pushing movement; When the shape of the stone is ellipsoid, the stone rotates to a certain extent before starting, and moves in the form of push when it reaches the starting speed; When the shape of the stone is nearly spherical, the movement form of the ballast is rolling. Because the rolling friction factor is smaller than the sliding friction factor, the starting speed of the nearly spherical ballast is smaller than that of the flat and ellipsoidal ballast. Because the ballast studied in this paper has a large size of equal volume, reaching 38.5 mm, it can't overcome gravity to make suspension movement under the action of mud buoyancy and turbulence. Generally, it makes push movement at the bottom of the pipeline, and when the ballast shape coefficient reaches above 0. 8, rolling will be the main movement form.

3.2 Influence of equal volume particle size on starting speed of stone

To investigate the effect of constant volume particle size on starting speed of stone particles, stones with shape coefficient of 0.4 and different constant volume particle sizes were placed in the pipeline. The movement speed of stones with different volume particle sizes is depicted in Fig. 10. It can be obtained from Fig. 10 that when the constant volume particle diameter D_V of ballast is 19.2 ~ 38.5 mm, the stone movement velocity curves are almost coincident.

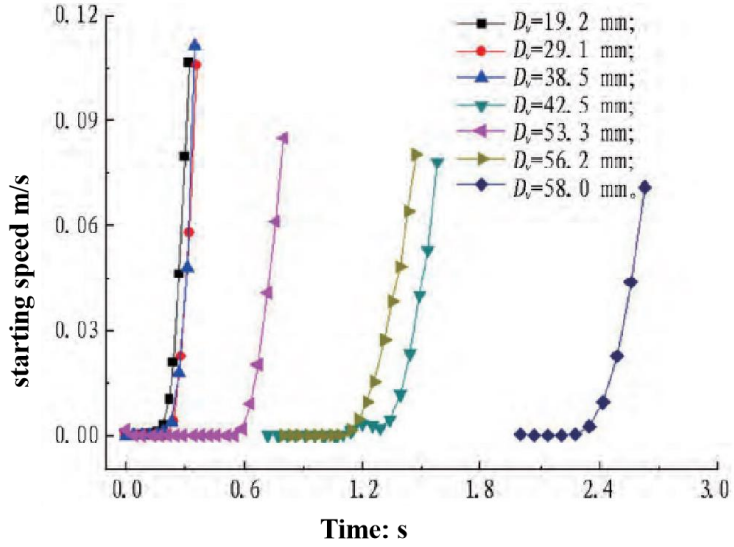


Figure 10. Velocity of a pebble with different equal volume particle sizes.

The starting speed of stones with different sizes of equal volume is shown in Fig. 11. From Fig. 11, it can be deduced that when the equal volume particle size of stone is small, the starting speed of stone is almost equal; When the equal volume diameter D_V of stone is 38. 5, 42.5, 53.3, 56.2 and 58 mm, the starting speed vi of stone is 0.48, 1.06, 1.26, 2.36 and 4.70 m/s, and the starting speed of adjacent equal volume diameter stones increases by 120.8%, 18.9%, 87.3% and 99.2%. When the stone volume particle size is less than 38.5 mm, the influence is not obvious. This is because as stone volume particle size increases, the friction resistance between the stone and the pipe wall is greater, and the required drag forces are also greater. At the same time, the drag force is proportional to the quadratic difference between the mud and the stone. The initial state of the stone is static at the lower section of the pipe wall, and its speed is 0 m/s, that is, the drag force is proportional to the quadratic of the mud speed. When the stone volume particle size is smaller, the required drag force is also smaller. Therefore, when the constant volume particle size is small, starting speed of the stone has little difference. When the constant volume particle size increases to a certain extent, the drag force required to push the stone to move obviously increases, and it shows an upward trend with the further increase in constant volume particle size.

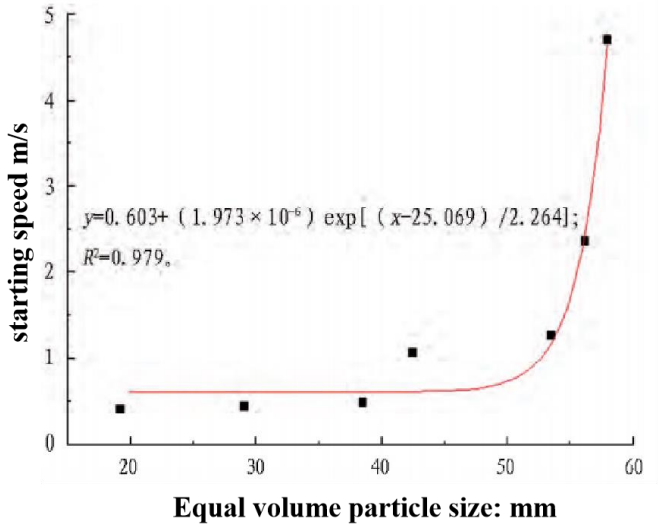


Figure 11. Starting speed of stone with different equal volume particle sizes.

4. Conclusions

In this study, combining CFD and DEM, this paper set up the movement model of the stone in the horizontal pipe of slurry shield circulating system, and studies the influence of stone shape coefficient and equal volume particle size on the starting speed of the stone. The main conclusions are as below:

Under the condition of equal volume particle size, the starting speed of different shapes of stones is ellipsoid > flat > nearly spherical. When the stone shape is flat and nearly spherical, the starting speed of stone is low; When the stone is ellipsoidal, it will rotate to a certain extent before reaching the starting speed, and the starting speed will jump when compared with the flat one. When S_f=0.55 compared with S_f = 0.37, the starting speed of the stone will reach 1.4 m/s, with an increase of 204%.

The starting speed of stone increases exponentially with increasing equal volume particle size. When the equal volume particle size of stone is less than 38.5 mm, the starting speed of stone is about 0. 48 m/s; When the size of the stone is 42.5 ~ 58.0 mm, the starting speed of the stone increases with increasing the stone size.

Acknowledgement

With the rapid development of urban underground space, slurry shield is widely used in the construction of urban space, slurry shield circulation system plays an indispensable role in the safety construction of slurry shield. In the process of transporting slag stone, slurry circulation system often appears some problems, such as slurry pipe blockage, slurry pipe wear and too large energy loss. Too large circulation velocity can cause excessive energy loss, and too small circulation velocity can cause blockage. Therefore, studying a suitable circulation speed has a guiding role in the actual construction.

I would like to express my sincere gratitude to Mrs Li who guided me through my research journey. With the help of her, the research topic was determined by consulting literature. In addition, she also guided my theoretical basis and technical answers, and helped me revise the drafts of my papers.

References

[1] Cheng, W. C., Bai, X. D., Sheil, B. B., Li, G., Wang, F., 2020. Identifying characteristics of pipejacking parameters to assess geological conditions using optimisation algorithm-based support vector machines. Tunn. Undergr. Space Technol. 106, 103592.

[2] Zhang, K., Lyu, H. M., Shen, S. L., Zhou, A., Yin, Z. Y., 2020. Evolutionary hybrid neural network approach to predict shield tunneling-induced ground settlements. Tunn. Undergr. Space Technol. 106, 103594.

[3] Yang, D., Xia, Y., Wu, D., Chen, P., Zeng, G., Zhao, X., 2018. Numerical investigation of pipeline transport characteristics of slurry shield under gravel stratum .Tunn. Undergr. Space Technol. 71, 223-230.

[4] Tan, Y., Zhang, H., Yang, D., Jiang, S., Song, J., Sheng, Y., 2012. Numerical simulation of concrete pumping process and investigation of wear mechanism of the piping wall. Tribology International, 46(1), 137-144.

[5] Zhang, H., Tan, Y., Yang, D., Trias, F. X., Jiang, S., Sheng, Y., Oliva, A., 2012. Numerical investigation of the location of maximum erosive wear damage in elbow: Effect of slurry velocity, bend orientation and angle of elbow. Powder Technology, 217, 467-476.

[6] Wu, D., Yang, B., Liu, Y., 2015. Transportability and pressure drop of fresh cemented coal gangue-fly ash backfill (CGFB) slurry in pipe loop. Powder Technology, 284, 218-224.

[7] Arolla, S. K., Desjardins, O., 2015. Transport modeling of sedimenting particles in a turbulent pipe flow using Euler–Lagrange large eddy simulation. International Journal of Multiphase Flow, 75, 1-11.

[8] Kaushal, D. R., Thinglas, T., Tomita, Y., Kuchii, S., Tsukamoto, H., 2012. CFD modeling for pipeline flow of fine particles at high concentration. International Journal of Multiphase Flow, 43, 85-100.

[9] Akhshik, S., Behzad, M., Rajabi, M., 2016. CFD-DEM simulation of the hole cleaning process in a deviated well drilling: The effects of particle shape. Particuology, 25, 72-82.

[10] Wang, Y., Xia, Y., Xiao, X., Xu, H., Chen, P., 2019. Ballast flow characteristics of discharging pipeline in shield slurry system. Applied Sciences. 9, 5402.

[11] Cundall, P. A., Strack, O. D., 1979. A discrete numerical model for granular assemblies. geotechnique, 29(1), 47-65.